STEM CELLS AND DEVELOPMENT
Volume 24, Number 14, 2015

DOI: 10.1089/scd.2014.0496

The Therapeutic Effects of Human Mesenchymal Stem Cells Primed with Sphingosine-1 Phosphate on Pulmonary Artery Hypertension

Hyunsook Kang,[1,2,*] Kang-Hyun Kim,[3,*] Jisun Lim,[1,2] You-Sun Kim,[3] Jinbeom Heo,[1,2] Jongjin Choi,[3] Jaeho Jeong,[1,2] YongHwan Kim,[1,2] Seong Who Kim,[4] Yeon-Mok Oh,[3] Myung-Soo Choo,[5] Jaekyoung Son,[1] Su Jung Kim,[6] Hyun Ju Yoo,[6] Wonil Oh,[7] Soo Jin Choi,[7] Sei Won Lee,[3] and Dong-Myung Shin[1,2]

Stem cell (SC) therapy has become a potential treatment modality for pulmonary artery hypertension (PAH), but the efficacy of human SC and priming effects have not yet been established. The mobilization and homing of hematopoietic stem cells (HSCs) are modulated by priming factors that include a bioactive lipid, sphingosine-1-phosphate (S1P), which stimulates CXCR4 receptor kinase signaling. Here, we show that priming human mesenchymal stem cells (MSCs) with S1P enhances their therapeutic efficacy in PAH. Human MSCs, similar to HSCs, showed stronger chemoattraction to S1P in transwell assays. Concomitantly, MSCs treated with 0.2 μM S1P showed increased phosphorylation of both MAPKp42/44 and AKT protein compared with nonprimed MSCs. Furthermore, S1P-primed MSCs potentiated colony forming unit-fibroblast, anti-inflammatory, and angiogenic activities of MSCs in culture. In a PAH animal model induced by subcutaneously injected monocrotaline, administration of human cord blood-derived MSCs (hCB-MSCs) or S1P-primed cells significantly attenuated the elevated right ventricular systolic pressure. Notably, S1P-primed CB-MSCs, but not unprimed hCB-MSCs, also elicited a significant reduction in the right ventricular weight ratio and pulmonary vascular wall thickness. S1P-primed MSCs enhanced the expression of several genes responsible for stem cell trafficking and angiogenesis, increasing the density of blood vessels in the damaged lungs. Thus, this study demonstrates that human MSCs have potential utility for the treatment of PAH, and that S1P priming increases the effects of SC therapy by enhancing cardiac and vascular remodeling. By optimizing this protocol in future studies, SC therapy might form a basis for clinical trials to treat human PAH.

Introduction

Pulmonary artery hypertension (PAH) is a rare disease characterized by the sustained elevation of pulmonary artery pressure and pulmonary vascular resistance, which ultimately leads to right heart failure and death [1]. Before the advent of novel therapies, the median survival of idiopathic PAH was estimated to be 2.8 years [2]. Over the past decade, the treatment of PAH has evolved considerably as a deeper understanding of the underlying pathogenesis has been gained [3–8]. However, despite these treatments, mortality remains high [8,9]. Therefore, there is a considerable unmet medical need in the management of PAH.

Mesenchymal stem cells (MSCs) are multipotent progenitor cells that have the ability to differentiate into bone, cartilage, muscle, or vascular smooth muscle cells, as well as other connective tissues [10–12]. Accumulating evidence suggests that stem cells (SCs), including MSCs, can be mobilized into the peripheral blood (PB) for recruitment to damaged organs where they can actively participate in tissue repair [13,14]. The beneficial effects of MSCs have also been attributed to paracrine factors, such as cytokine-dependent cytoprotective effects [15] and proangiogenic and proarteriogenic effects [16]. Based on these observations, MSC therapy has been investigated and applied to various therapeutically intractable diseases, including PAH. MSC injection can attenuate the pulmonary vascular structural and hemodynamic changes caused by PAH in various models [17,18]. This efficacy can be explained by several mechanisms. The most comprehensive pathogenesis of idiopathic

Departments of [1]Biomedical Sciences, [2]Physiology, [3]Pulmonary and Critical Care Medicine, and Clinical Research Center for Chronic Obstructive Airway Diseases, [4]Biochemistry and Molecular Biology, [5]Urology, and [6]Biomedical Research Center, Asan Medical Center, University of Ulsan College of Medicine, Seoul, Korea.
[7]Biomedical Research Institute, Medipost Co., Ltd., Seoul, Korea.
*These two authors contributed equally to this work.

PAH includes endothelial damage associated with increased blood coagulability, platelet aggregation, and vasoconstriction [19,20]. Inflammation also plays a prominent detrimental role in animal and human PAH [21]. MSCs have shown the multipotent ability to become endothelial progenitor cells [22,23] and also secrete a variety of growth factors, such as vascular endothelial growth factor (VEGF) [24]. MSC delivery can decrease lung inflammation in various diseases models [25,26]. Therefore, MSC administration appears to have enough evidence in PAH treatment. However, extremely rare engraftment of the injected MSCs persisting in the lungs should be overcome for clinical application of MSC therapy.

Some chemokines [*eg*, stromal cell-derived factor-1 (SDF-1)] and growth factors [*eg*, VEGF, basic fibroblast growth factor (bFGF), or hepatocyte growth factor (HGF)] play crucial roles in the mobilization and engraftment of adult SCs [27–32]. Among these chemotactic factors, SDF-1 and its receptor, CXCR4, can trigger a signaling cascade that has been established to be a central pathway in SC migration [27,28]. Interestingly, the responsiveness of stem cells to a chemotactic gradient of SDF-1 could be sensitized by molecules enriched in damaged tissues. This phenomenon is known as ''priming'' and has been well established in the process of hematopoietic stem/progenitor cell (HSPC) mobilization and engraftment [33]. Priming molecules stimulate the incorporation of CXCR4 receptor kinase into membrane lipid rafts, which thereby make physiologically lower doses of SDF-1 become ''more biologically significant'' in stem cell trafficking. The priming factors include bioactive lipids, such as sphingosine-1-phosphate (S1P) [34] and ceramide-1-phosphate (C1P) [35,36], in addition to complement C3 cleavage fragments (C3a and $_{\text{desArg}}$C3a) [37,38], soluble membrane attack complex C5b-9 [35], and cationic antimicrobial peptides, such as cathelicidin (LL-37) and β2-defensin released from activated granulocytes [39,40]. However, whether priming can occur other adult SCs, including MSCs, has been poorly characterized. Particularly, levels of S1P or antimicrobial peptide, hepcidin are increased in lung tissues or plasma of patients with PAH [41,42]. Here, we investigated the role of a bioactive lipid, S1P, and a cationic peptide, LL-37, on the priming of MSCs, a type of nonhematopoietic stem cell that has been in SC therapeutics. Furthermore, we show the beneficial function of MSC priming under in vivo conditions using an experimental PAH model.

Methods

Culturing human MSCs

Human adipose-derived MSCs (hAD-MSCs) were purchased from Invitrogen (Carlsbad, CA) and were cultured as previously described [43]. Human cord blood-derived MSCs (hCB-MSCs) used in this study were donated by Medipost Co., Ltd., (Seoul, Korea). hCB-MSCs were separated as described previously [44,45] and were maintained in high-glucose Dulbecco's modified Eagle's medium (DMEM; Hyclone, Pittsburgh, PA) supplemented with 2 mM L-glutamine, 20 mM HEPES (pH 7.3), MEM nonessential amino acid solution, penicillin/streptomycin (Cellgro, Pittsburgh, PA), 1 μg/mL ascorbic acid (Sigma-Aldrich, St. Louis, MO), 10% heat-inactivated fetal bovine serum (FBS; Hyclone), 5 ng/mL human epidermal growth factor, 10 ng/mL bFGF, and 50 μg/mL Long R3-insulin-like growth factor-1 (Prospec, Rehovot, Israel) in a humidified atmosphere with 5% CO_2 at 37°C. All MSCs were expanded for five passages to ensure multipotency. To analyze cell surface epitope expression characteristic to MSCs [46], 5.0×10^5 hAD- or hCB-MSCs were resuspended in DMEM containing 2% FBS and were stained with antibodies for 30 min on ice, washed twice, and then analyzed using a BD FACS Canto II flow cytometer (BD Biosciences, Mountain View, CA). The following fluorophore conjugated anti-human surface marker antibodies were purchased from BD Pharmingen (San Diego, CA): CD14 (FITC conjugated, clone M5E2), CD29 (PE, clone MAR4), CD34 (PE, clone 581), CD45 (PE, clone HI30), CD49f (FITC, clone GoH3), CD73 (PE, clone AD2), CD105 (APC, clone 266), and CD184/CXCR4 (FITC, clone 12G5). All data were analyzed with FlowJo software (Tree Satr, Inc., Ashland, OR).

Cell migration assay

Polycarbonate membranes that were 8 μm thick were coated with 50 μL 1.0% gelatin (Sigma-Aldrich) for 1 h. The MSCs detached with trypsin-ethylenediaminetetraaceticacid were washed and resuspended in DMEM containing 0.5% bovine serum albumin (BSA), and then were seeded at a density of 3×10^4 cells/well into the upper chambers of Transwell inserts (Costar Transwell; Corning Costar, Corning, NY). The lower chambers were filled with the indicated concentration of S1P (Cayman Chemical, Ann Arbor, MI) or LL-37 (ANASPEC, Fremont, CA) in 0.5% BSA DMEM. After 24 h, inserts were removed from the Transwell plates. Cells remaining in the upper chambers were scraped off with cotton wool, and the cells that had transmigrated were fixed with 4% paraformaldehyde solution in phosphate-buffered saline (PBS) and stained with 0.5% crystal violet (Sigma-Aldrich). Stained cells on the lower side of the membranes were quantified by digital image analysis using Image Pro 5.0 software (Media-Cybernetics, Rockville, MD).

Cell proliferation and colony forming unit-fibroblast assays

Cell proliferation after treatment with S1P or LL-37 for the indicated times was determined using the MTT assay (Sigma-Aldrich) according to the manufacturer's protocol. Reduction of the MTT reagent was performed for 4 h and quantified by measuring the absorbance at 570 nm using a microplate spectrophotometer (Molecular Devices, Sunnyvale, CA). For the colony forming unit-fibroblast (CFU-F) assay, MSCs were treated with S1P or LL-37 for 1 day and cells were replated at a clonal density (60 cells per each well) in six-well culture plates, and then were cultured in hCB-MSC media for 14 days. The established colonies were washed twice with PBS, fixed, and stained with 0.5% crystal violet (Sigma-Aldrich).

In vitro differentiation assays

In vitro differentiation into osteogenic, chondrogenic, or adipogenic lineages was performed as described previously [47]. Briefly, cells were maintained under normal growth medium and cultured in adipogenic (DMEM supplemented

with 5% FBS, 1 μM dexamethasone, 10 μM insulin, 200 μM indomethacin, and 0.5 mM isobutylmethylxanthine), osteogenic (DMEM supplemented with 5% FBS, 50 μM L-ascorbate-2-phosphate, 0.1 μM dexamethasone, and 10 mM glycerophosphate), or StemPro® chondrogenesis (Invitrogen) differentiation medium. Adipogenic differentiation was characterized by the accumulation of intracellular lipid, which could be visualized by Oil red O staining, and osteogenic differentiation was noted by positive staining with Alizarin Red, which is specific for calcium. The chondrogenic differentiation was examined by Alcian Blue staining.

Anti-inflammation and angiogenesis assays for MSCs

For anti-inflammation assay, we employed the cell-based bioassay to measure the secretion of tumor necrosis factor (TNF)-α from MH-S, a murine alveolar macrophage cell line in the response to lipopolysaccharides (LPS) stimulation [48]. MH-S was maintained in high-glucose DMEM supplemented with 10% heat-inactivated FBS and penicillin/streptomycin. About 1×10^5 MH-S cells were seeded in a 12-well culture plate, followed by stimulation with 0.1 μg/mL LPS (Sigma-Aldrich) in the absence or presence of conditioned medium (CM), which was harvested from IMR90 or hCB-MSCs after treatment with 0.2 μM S1P or 2.5 μM LL-37 for 1 day. After 5 h, medium conditioned by MH-S macrophages was collected and clarified by centrifugation at 500 *g* for 10 min. A 50 μL aliquot of MH-S medium was assayed using a murine TNF-α ELISA kit (Thermo Scientific, Pittsburgh, PA). For the angiogenesis assay, we evaluated the effect of CM from hCB-MSCs on the proliferation of human umbilical vein endothelial cells (HUVEC) [49]. HUVEC (Lonza, Inc., Cleveland, TN) was maintained in EGM™ medium according to the manufacturer's instruction. About 5×10^3 HUVEC cells seeded in a 96-well culture plate were starved with 1% serum containing medium for 24 h and then stimulated with CM harvested from the indicated cells. Cell proliferation at the indicated days after treatment of CM was determined using the MTT assay (Sigma-Aldrich) according to the manufacturer's instruction. Reduction of the MTT reagent was performed for 4 h and quantified by measuring the absorbance at 570 nm using a microplate spectrophotometer (Molecular Devices).

Western blot

MSCs were starved for 1 day in DMEM containing 0.5% BSA at 37°C, stimulated with the indicated concentration of S1P or LL-37 for 5 or 10 min, and then were lysed for 30 min on ice in RIPA lysis buffer containing protease and phosphatase inhibitors (Santa Cruz Biotechnology, Santa Cruz, CA). Cell extracts (30 μg) were separated using 12% sodium dodecyl sulfate–polyacrylamide gel electrophoresis gels and analyzed for the phosphorylation of $MAPK^{p42/44}$ and AKT (Ser473) (Cell Signaling Technology, Danvers, MA). Equal loading was confirmed using monoclonal or polyclonal antibodies against total MAPKp44/42 and total AKT (Cell Signaling Technology).

PAH animal model

Male specific-pathogen-free Lewis rats (8 weeks, 250–280 g) were raised under a controlled room temperature and lighting (12 h light–dark cycle) with free access to food and water. PAH was induced by the subcutaneous injection of monocrotaline (MCT, 60 mg/kg; Sigma-Aldrich). Rats in the control group were injected with the same volume of PBS. Two weeks after MCT or PBS injection, hCB-MSCs without priming or pretreated with 0.2 μM S1P for 3 h (S1P-MSC) were injected via the tail vein at a density of 2.5×10^5 cells per 200 μL PBS. For a vehicle control, same volume of (200 μL) PBS without cells was injected. Before infusion, cells were washed with warm PBS twice and the viability of injected cells was monitored by the excluded staining of 7-AAD (BD Biosciences) by FACS analysis (Supplementary Fig. S1; Supplementary Data are available online at www.liebertpub.com/scd).

Measurement of right ventricular systolic pressure and right ventricular hypertrophy

Four weeks after MCT or PBS injection, the right ventricular systolic pressure (RVSP) was measured via direct puncture through the diaphragm using a 26G needle connected to a patient monitor (MDE Escort II patient monitor, Arleta, CA) under breathing with the ventilator (Harvard Apparatus inspira asv, Holliston, MA) and anesthesia with zoletil (40 mg/kg) and rompun (10 mg/kg), as described previously [50]. Right ventricular pressure was maintained to allow breathing with a ventilator. To determine the right ventricular hypertrophy, the right ventricle (RV) of the heart was separated from the interventricular septum, and the weights of the RV and left ventricle (LV), including the interventricular septum (LV + S), were measured.

Histological analysis

Randomly selected vessels, with a diameter of 25–100 μm in hematoxylin and eosin- or α-smooth muscle actin (α-SMA)-stained sections of 4 μm thickness, were captured at 400× magnification in at least five randomly selected fields. To quantify the density of blood vessels, the sections stained with rat RECA-1, a cell surface antigen that is expressed by all rat endothelial cells were also examined. Anti-Rat RECA-1 (1:100; Abcam, Cambridge, United Kingdom) and anti-α-SMA (1:100; Abcam) were applied and incubated according to the manufacturers' recommended protocols. Medial wall thickness was measured as previously described [51] using the NIH ImageJ program (http://rsbweb.nih.gov/ij/). The medial wall thickness index was defined as a ratio of the external diameter–internal diameter to the external diameter.

Reverse transcriptase and real-time quantitative polymerase chain reaction

Total RNA from MSCs was isolated using an RNeasy-Mini Kit (Qiagen, Inc., Valencia, CA), and genomic DNA was removed using the DNA-free Kit (Applied Biosystems, Foster City, CA). Then, mRNA (400 ng) was reverse transcribed using TaqMan Reverse-Transcription Reagents (Applied Biosystems), according to the manufacturer's instructions. Quantitative assessments of the expression levels of adipogenic or osteogenic lineage genes were performed using real-time quantitative polymerase chain reaction

(RQ-PCR) with the PikoReal™ Real-Time PCR System (Thermo Scientific) with SYBR Green PCR Master Mix (Applied Biosystems), as described previously [52].

S1P measurement

One million of hCB-MSCs were lysed using methanol and lipids were extracted by Bligh and Dyer procedures. One hundred nanomolar C17 ceramide (Sigma-Aldrich) is used as an internal standard and added during the initial step of lipid extraction. S1P content was determined performed using liquid chromatography-tandem mass spectrometry system equipped with Agilent 1290 HPLC (Agilent, Santa Clara, CA), Qtrap 5500 (ABSciex, Framingham, MA) and reverse phase column (Pursuit 5 C18 150×2.0 mm). The multiple reaction monitoring mode was used in the negative ion mode and the peak area of the extracted ion chromatogram corresponding to the specific transition for each lipid was used for quantification. Data

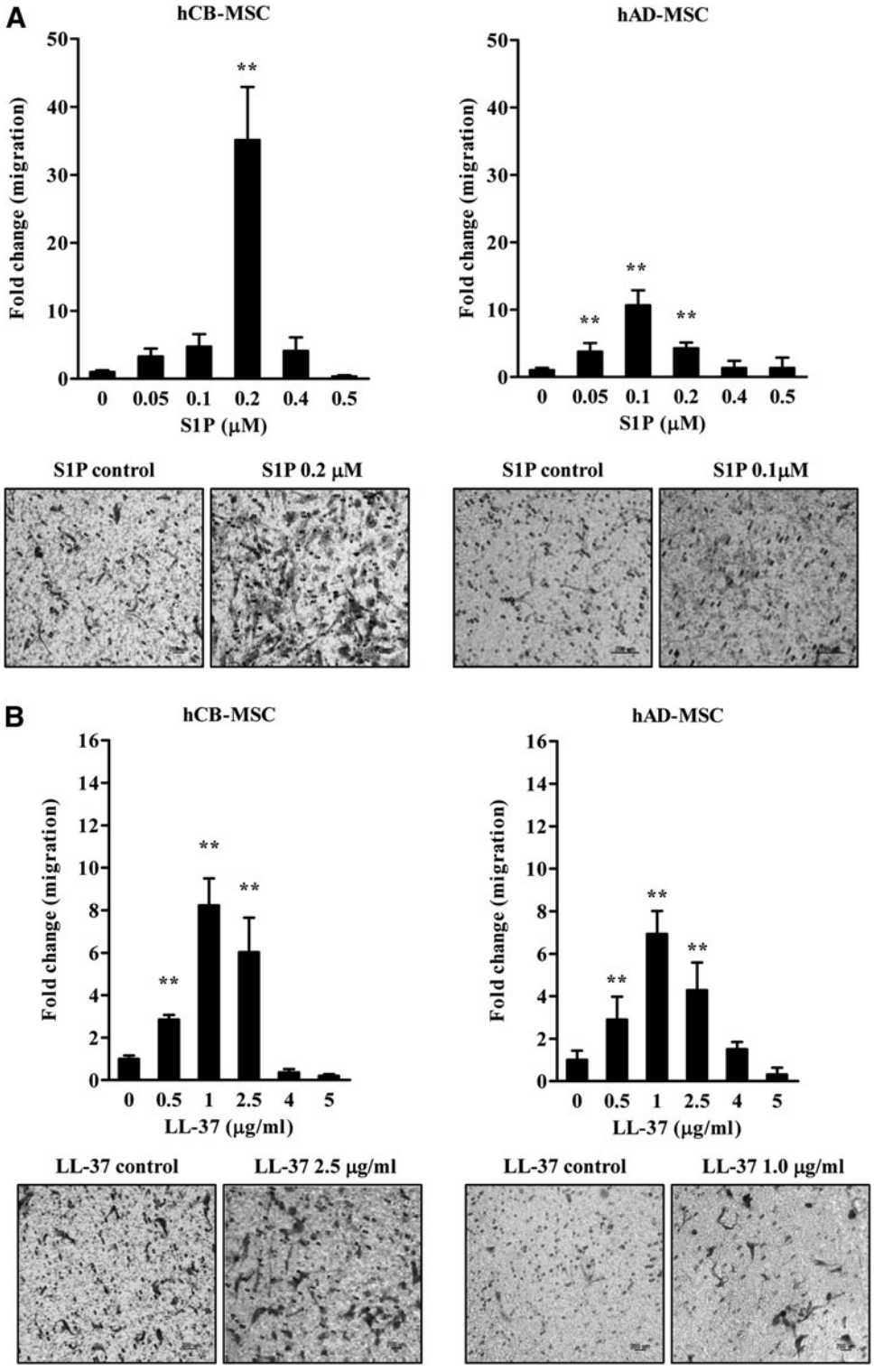

FIG. 1. Enhanced mesenchymal stem cell (MSC) migration in response to sphingosine-1-phosphate (S1P) and LL37. Chemotaxis assays of human cord blood (hCB) or adipose-derived (hAD) MSCs exposed to the indicated concentrations of S1P **(A)** or LL-37 **(B)**. The relative amount of migration is shown as the fold-change compared to the number of cells that transmigrated; mean ± standard deviation (SD) from at least eight independent experiments are indicated; $^{**}P < 0.01$, compared to cells in the absence of S1P [one-way analysis of variance (ANOVA) with Bonferroni post-test]. Representative images for transwell *insets* from the migration assay are shown in the *lower panel* for the indicated MSCs. Control indicates medium alone.

analysis was performed by using Analyst 1.5.2 software. Calibration range for S1P was 1–1,000 nM ($r^2 \geq 0.99$). S1P level was normalized to total protein content in the samples.

Statistical analysis

Data were analyzed using Student's *t*-test or one-way analysis of variance with the Bonferroni post hoc test to detect statistically significant differences. We used GraphPad Prism 5.0 software (GraphPad Software, La Jolla, CA) to perform all analyses, and statistical significance was defined as $P < 0.05$ or 0.01.

Study approval

All animal experiments were approved by the Institutional Animal Care and Use Committee of the University of Ulsan College of Medicine (IACUC-2014-12-073). Umbilical cord bloods were collected from umbilical veins after neonatal delivery with the informed consent of the mothers.

Results

S1P and LL-37 enhance the migratory activity of hAD- and hCB-MSCs

We attempted to investigate the effects of S1P and LL-37 on the cellular properties of human MSCs derived from different tissues. To address this issue, we first examined whether these priming molecules, which can affect the mobilization and homing of HSPCs [34,35], could chemoattract hCB- or hAD-derived MSCs. To test the chemotatic effects S1P and LL-37 on these cells, we employed a transwell migration assay; both factors significantly stimulated the migratory activity of both MSCs (Fig. 1). Notably, hCB-MSCs showed superior migration activity compared with hAD-MSCs, and S1P enhanced chemoattraction more than LL-37 (Fig. 1). Thus, hCB-MSCs pretreated with 0.2 μM S1P show the highest increase (~40-fold) in chemotatic activity (Fig. 1A).

S1P and LL-37 accelerates signal transduction in MSCs

Next, to further characterize the priming effect of S1P and LL-37 that we observed in the chemotaxis assay, we evaluated the status of the signaling pathways implicated in the migration of HSPCs [34,35,39,40]. The hCB-MSCs exposed to S1P or LL-37 showed activation of both the MAPK and AKT pathways, as indicated by increased phosphorylation of the MAPKp42/44 and AKT proteins (Fig. 2A). In hAD-MSCs, priming with S1P or LL37 increased the phosphorylation of only AKT protein, but did not affect the MAPK pathway (Fig. 2B). Altogether, these results indicate that S1P and LL37 priming molecules can enforce the migratory activity of several types of adult SCs including HSPCs by activating similar signaling pathways [34,39].

The effect of S1P or LL-37 on the basic characteristics of MSCs

Next, we test whether basic characteristics of MSCs could be affected by the treatment of S1P or LL-37. The multipotent MSCs express CD29, CD73, and CD105 surface molecules but lack expression of CD14, CD34, and CD45 hematopoietic lineage markers [46]. Exposure to S1P or LL-37 had little effect on the expression of surface marker proteins that define MSC and other molecules (CXCR4 and

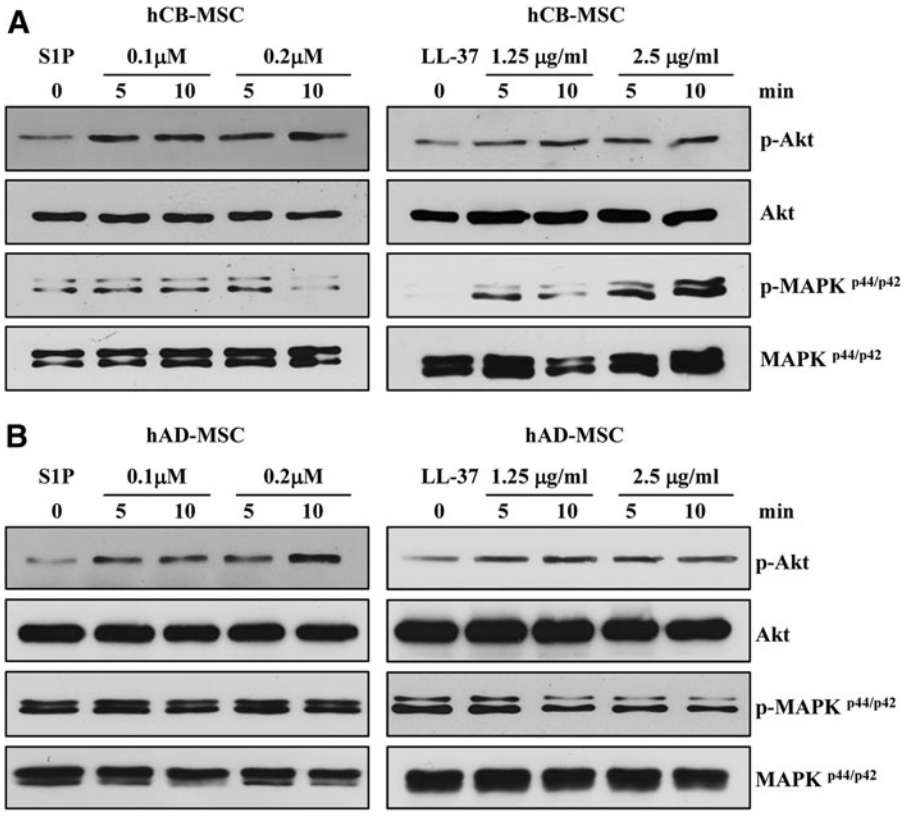

FIG. 2. Signaling pathway activation in MSCs primed with S1P or LL37. Priming can activate two signaling pathways in hCB-MSCs **(A)** and hAD-MSCs **(B)** that are implicated in hematopoietic stem/progenitor cell migration, MAPKp42/44 and AKT. MSCs were starved overnight in Dulbecco's modified Eagle's medium containing 0.5% bovine serum albumin and were treated with S1P (0.1 or 0.2 μM) or LL-37 (1.25 or 2.5 μg/mL) for 5 or 10 min.

CD49f) that are characteristic to primitive MSCs [47] (Fig. 3A; Supplementary Fig. S2). Additionally, S1P- or LL-37-mediated hCB-MSC priming had little effect on the capacity for cell proliferation (Fig. 3B) or in vitro differentiation into the adipogenic, chondrogenic, and osteogenic lineages, which were estimated by an increased level of accumulation (Oil Red O staining), cartilage proteoglycans (Alcian Blue staining), and mineral deposition (Alizarin Red S staining), respectively (Fig. 3C). We found that the coordinated induction of adipogenic (*eg*, *PPAR-γ*, *LEP/leptin*, and *FABP4/aP2*) or ostenogenic (*eg*, *RUNX2*, *OCN*, and *osteocalcin*) genes was independent or S1P or LL-37 priming (Fig. 3D). The S1P priming decreased the induction of some chondrogenic genes (*ACAN* and *COL10A1*) (Fig. 3D). Based on our data, we demonstrate that the treatment of S1P or LL-37 has little effect on the basic features of MSCs.

The priming with S1P improves the therapeutic potency of hCB-MSCs

Next, we examined whether the priming molecules could affect the characteristics of MSCs that influence their therapeutic potency. Importantly, hCB-MSC treated with S1P increased the capacity of clonogenic CFU-F, which indicates the presence of true clonogenic progenitor cells, and this activity peaked at 0.2 μM (Fig. 4A). Increased numbers of CFU-F were also observed in LL-37-primed hCB-MSCs. Since MSCs can suppress inflammatory responses, we next attempted to compare the anti-inflammatory effect of priming MSCs with S1P. To address this, we pretreated MH-S alveolar macrophages cells with LPS, and then examined whether the secretion of TNF-α from MH-S cells could be suppressed in the presence of CM collected from hCB-MSCs primed with S1P. CM from hCB-MSCs reduced TNF-α secretion from the LPS-stimulated alveolar macrophage cell line (Fig. 4B), which was consistent with previous reports [53]. Notably, the anti-inflammatory capacity was further enhanced in CM from S1P-primed MSCs. By contrast, CM collected from IMR90 cells, a type of human lung fibroblast, showed little effect in our in vitro inflammation assays. When we examined the expression of proinflammation cytokines and anti-inflammatory factors secreted by MSCs [48], the treatment of S1P increased the transcripts of anti-inflammatory genes such as *TSG6* and *LIF*, however, it repressed the expression of several proinflammatory cytokines including *CCL2*, *IL1B*, *IL6*, and *IL12A* (Fig. 4C; Supplementary Fig. S3A). The

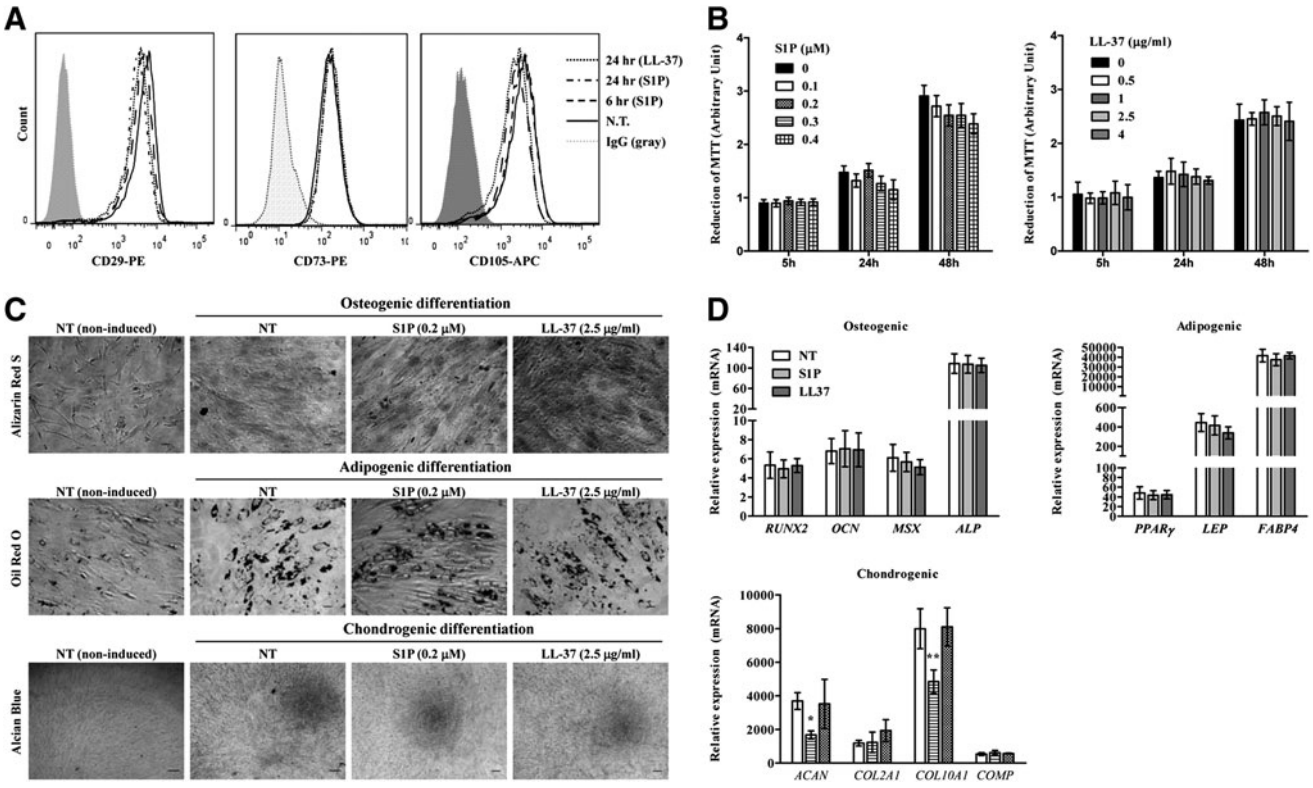

FIG. 3. The effect of S1P or LL-37 on the properties of MSCs. **(A)** Flow cytometry analysis of the expression of MSC surface proteins (CD29, CD73, and CD105) using hCB-MSCs after treatment with 0.2 μM S1P or 2.5 μg/mL LL-37 for the indicated amount of time. **(B)** Cell proliferation analysis of hCB-MSCs exposed to the indicated dose and duration of S1P (*left panel*) or LL-37 (*right panel*). **(C)** hCB-MSCs after treatment with 0.2 μM S1P or 2.5 μg/mL LL-37 for 1 day were differentiated by culture in osteogenic (*upper panel*), adipogenic (*middle panel*), or chondrogenic (*lower panel*) induction media. Osteogenesis, adipogenesis, and chondrogenesis were determined using Alizarin Red S, Oil Red O, and Alcian Blue staining, respectively. **(D)** Real-time quantitative polymerase chain reaction (RQ-PCR) analysis of the induction of osteogenic, adipogenic, and chondrogenic genes in hCB-MSCs. The relative expression level of the indicated genes is represented as the fold-change compared to the value of MSCs cultured under noninducing medium and are shown as mean ± SD of three independent experiments. $*P < 0.05$, $**P < 0.01$ compared to N.T. (one-way ANOVA with Bonferroni post-test). NT, non-treated.

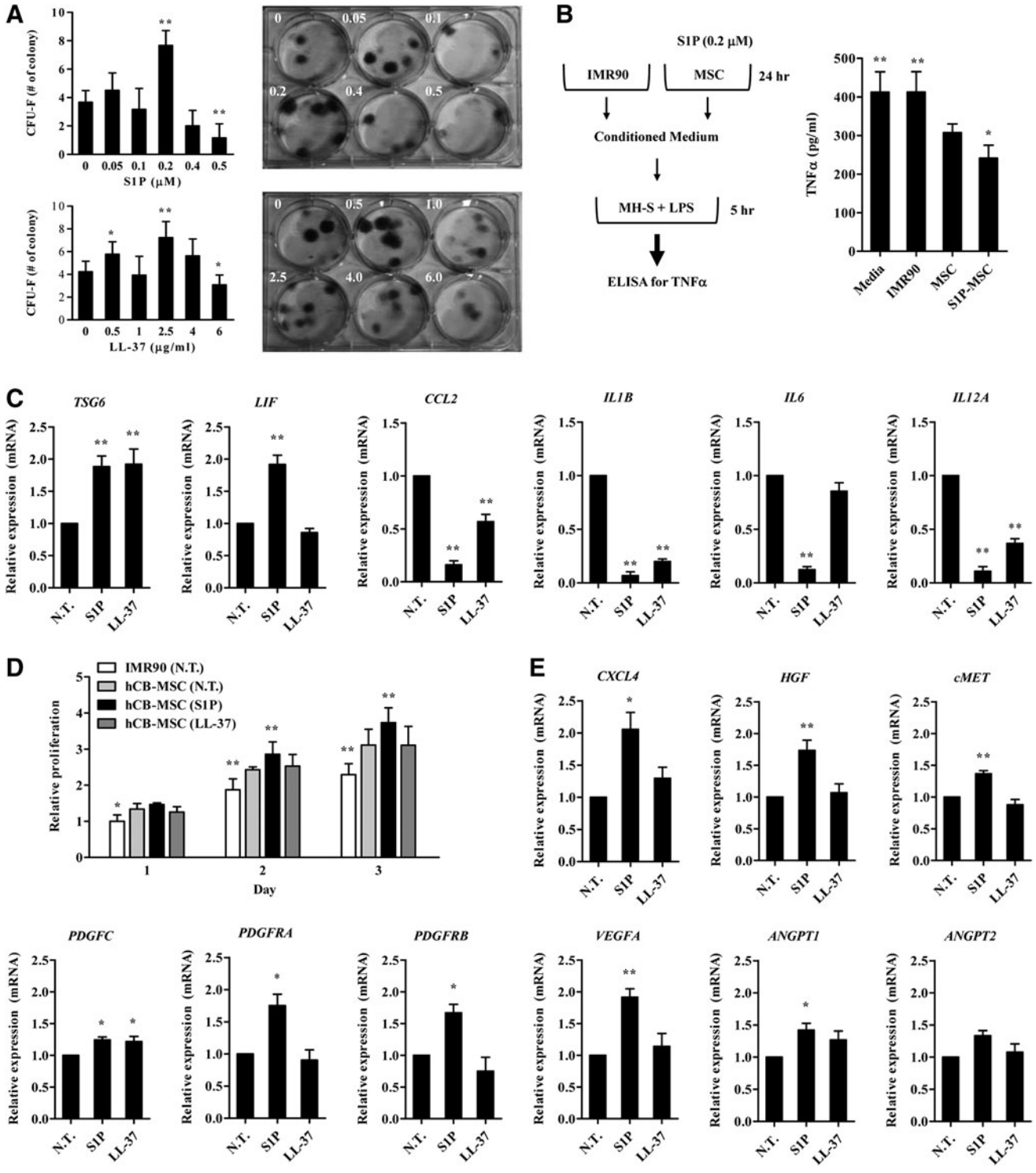

FIG. 4. Enhanced therapeutic potency of S1P primed hCB-MSCs. **(A)** hCB-MSCs were prestimulated with the indicated dose of S1P or LL-37. After 1 day, 60 cells were seeded into six-well culture plates and cultured for 14 days in complete medium. The number of colonies was counted and are presented as the mean ± SD ($n \geq 8$); $^{*}P < 0.05$, $^{**}P < 0.01$, compared to cells in medium alone (one-way ANOVA with Bonferroni post-test). Representative stained colonies of adherent cells are shown in the *right panel*. **(B)** A schematic diagram for the in vitro anti-inflammatory activity assay (*left panel*). Quantification of tumor necrosis factor-α protein secreted from a murine alveolar macrophage cell line stimulated with lipopolysaccharides (LPS) for 5 h in the absence or presence of conditioned medium (CM) harvested from the indicated cells. Data are presented as mean ± SD ($n = 9$); $^{*}P < 0.05$, $^{**}P < 0.01$ compared to media alone (one-way ANOVA with Bonferroni post-test). S1P-MSC indicates hCB-MSC primed with 0.2 μM S1P for 1 day. **(C, E)** RQ-PCR analysis of the inflammation- **(C)** and angiogenesis-related **(E)** genes in hCB-MSCs after treatment with 0.2 μM S1P or 2.5 μg/mL LL-37 for 24 h. The relative expression level of the indicated genes is represented as the fold change compared to the value of MSCs cultured without priming (N.T.) and are shown as mean ± standard error of mean (SEM, $n = 5$); $^{**}P < 0.01$ compared to N.T. (one-way ANOVA with Bonferroni post-test). **(D)** Cell proliferation analysis of human umbilical vein endothelial cells at the indicated days after treatment of CM harvested from the indicated cells. Fold differences relative to IMR90 at 1 day are shown as the mean ± S.D. ($n = 10$), ($^{*}P < 0.05$, $^{**}P < 0.01$ compared to N.T.).

changed expression of these genes were also observed in hCB-MSCs primed with LL-37.

Stimulation of angiogenesis is crucial for the beneficial outcome of the MSC therapy targeted to PAH [19,20]. To test whether the S1P priming can improve the angiogenesis potency of hCB-MSCs, we examine proangiogenic activity of the primed MSCs employing endothelial cell proliferation assays. As shown in Fig. 4D, CM from hCB-MSCs primed with S1P, but not LL-37, significantly increased the proliferation of HUVEC cells. Accordingly, the S1P priming upregulated several proangiogenic factors and their cognate receptors including CXCR4, HGF, platelet-derived growth factor (PDGF), VEGFA, and angiopoietin 1 (ANGPT) (Fig. 4E; Supplementary Fig. S3B). Taken together, our results in these cell culture models indicate that priming with S1P can improve migration, self-renewal, anti-inflammatory, and angiogenic capacity of MSCs, which is crucial for their therapeutic potency.

S1P-mediated enhancement of the therapeutic capacity of MSCs in a PAH animal model

Next, we attempt to examine the effect of MSC priming under in vivo conditions using a PAH animal model induced by MCT. Similar to a previous report [17], RVSP was significantly increased 4 weeks after MCT injection (42.0 ± 7.4 mmHg vs. 21.6 ± 2.6 mmHg, $P < 0.001$). Both injection of hCB-MSC (32.4 ± 4.0 mmHg, $P < 0.01$) or hCB-MSC primed with S1P (S1P-MSC, 30.1 ± 4.4 mmHg, $P < 0.001$) significantly attenuated MCT-induced RVSP elevation (Fig. 5A). RV/(LV + S) also increased after MCT injection. S1P-MSC significantly reduced this RV hypertrophy, but hCB-MSC without priming failed to cause a significant reduction (Fig. 5B). S1P-MSC injection also attenuated the increase of the medial wall thickness index and α-SMA$^+$ smooth muscle cells induced by MCT injection (Fig. 5C, D). Additionally, hCB-MSC without priming slightly lowered the vessel wall thickness index, but this difference did not reach our threshold for statistical significance (Fig. 5C). We also examined hAD-MSCs in this PAH model, but they did not show any significant improvement in RVSP, RV/(LV + S), or the vessel wall thickness index (data now shown).

When we stained human mitochondria in lung tissues, we failed to detect antigen-positive cells in any of the lung tissues tested (data not shown). To exclude low sensitivity immunostaining, we also used a sensitive PCR-based assay to detect human *Alu* element DNA sequences. However,

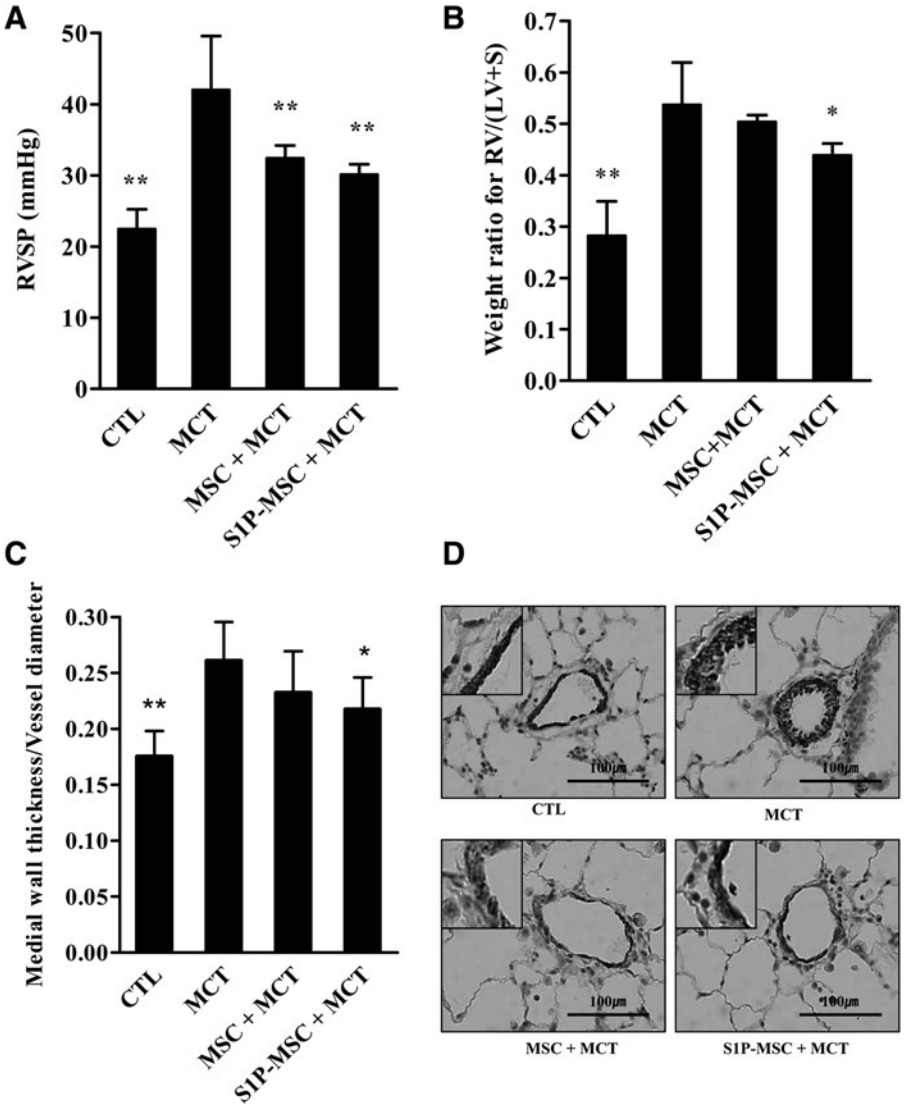

FIG. 5. The effects of hCB-MSCs and S1P-primed MSCs (S1P-MSC) for monocrotaline (MCT)-induced pulmonary artery hypertension in rats. **(A)** MCT induced increased levels of right ventricular systolic pressure (RVSP) (42.0 ± 7.4 mmHg vs. 21.6 ± 2.6 mmHg, $P < 0.001$), and hCB-MSC and S1P-MSC injection at 2 weeks after MCT injection significantly attenuated this elevation (32.4 ± 4.0 mmHg, $P < 0.01$ and 30.1 ± 4.4 mmHg, $P < 0.001$, respectively). **(B)** MCT increased the weight ratio for right ventricle (RV)/left ventricle (LV + S) and S1P-MSC significantly attenuated this effect. **(C)** MCT increased the medial wall thickness index (vessel wall thickness per vessel diameter), and S1P-MSC significantly attenuated this increase. hCB-MSC without priming failed to show significant improvements in RV/(LV + S) and medial wall thickness index. **(D)** Immunohistochemical detection of α-smooth muscle actin (SMA) + smooth muscle cells in pulmonary vessel (magnification, 400×). RVSP, right ventricular systolic pressure; CTL, control; MSC, human cord blood mesenchymal stem cell; S1P-MSC, sphingosine-1-phosphate primed human cord blood mesenchymal stem cell; LV + S, left ventricle and interventricular septum. *$P < 0.05$, **$P < 0.01$ compared to MCT alone (one-way ANOVA with Bonferroni post-test). S1P-MSC indicates hCB-MSC primed with 0.2 μM S1P for 3 h before injection.

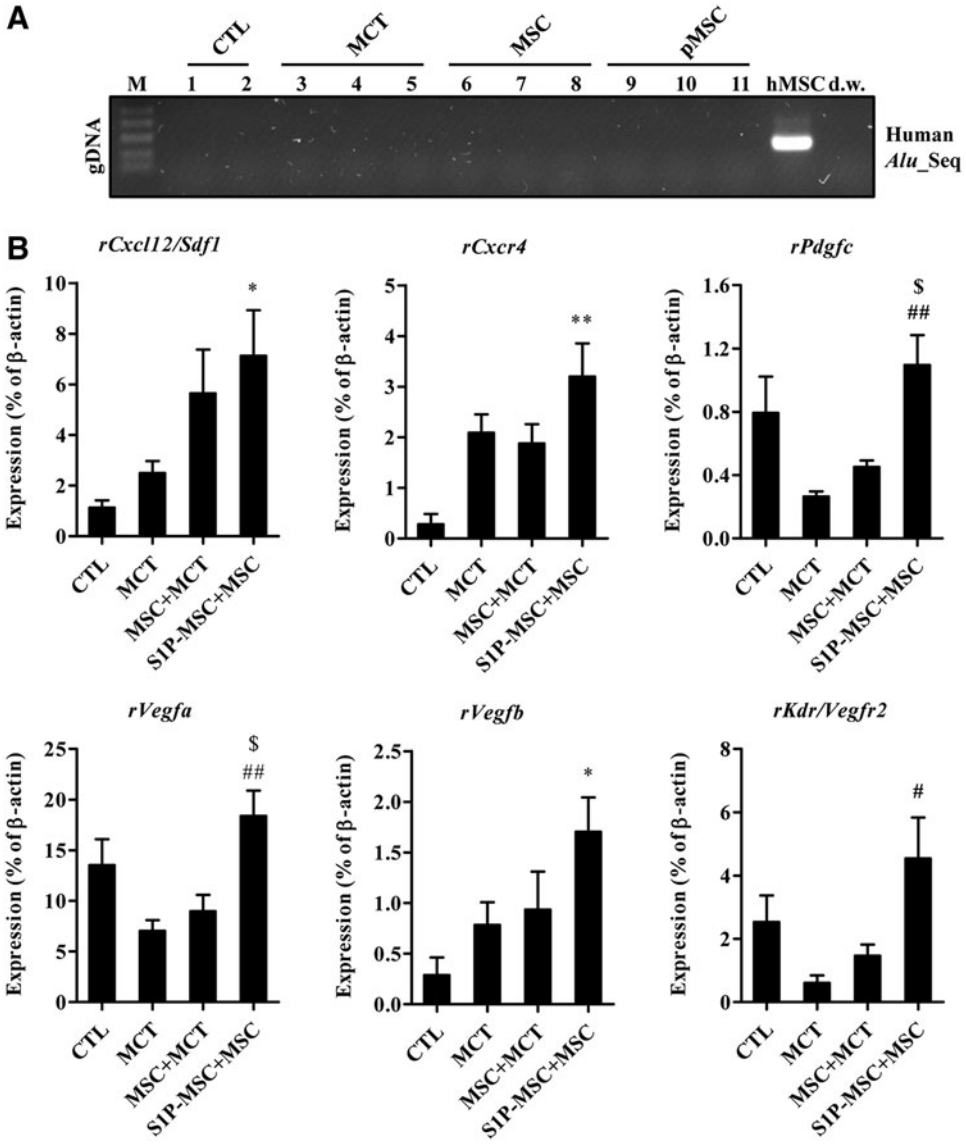

FIG. 6. Increased expression of genes encoding stem cell trafficking markers and angiogenesis factors in lungs injected with S1P-primed MSC. **(A)** PCR analysis for the detection of human *Alu* element sequences (*Alu*_Seq) in lung tissues from the indicated groups; dw, distilled water. **(B)** RQ-PCR analysis of genes involved in stem cell migration and angiogenesis (*ie*, chemokines, growth factors, and their receptors) in lungs from the indicated groups. The relative expression levels of *Sdf1/Cxcl12*, *Cxcr4*, *Pdgfc*, *Vegfa*, *Vegfb*, and *Kdr/Vegfr2* are presented as the fold-change relative to the value for the control rats (CTL) and are shown as mean ± SEM ($n = 4$; $^{*}P < 0.05$, $^{**}P < 0.01$ compared with CTL), $^{\#}P < 0.05$, $^{\#\#}P < 0.01$ compared with MCT, $^{\$}P < 0.05$ compared with MSC + MCT.

human DNA-specific sequences were not observed (Fig. 6A), suggesting that S1P priming might be insufficient for enhancing the engraftment of systemically injected MSCs. Thus, we hypothesized that MSC priming can enforce the paracrine effects of MSCs [54–56], and we performed RQ-PCR analysis to determine the expression levels of genes involved in SC trafficking and angiogenesis [43]. The lung tissues in the S1P-MSC group exhibited the highest level of transcripts for rat *Cxcl12/Sdf1* and *Cxcr4* (Fig. 6B). Furthermore, the lung tissues from rats injected with S1P-MSC highly expressed a subtype of angiogenic factors, including *Pdgfc*, *Vegfa*, *Vegfb*, and *Kdr/Vegfr2*. Since the S1P priming enhanced the in vitro angiogenesis capacity (Fig. 4D) and upregulated some proangiogenic factors (Fig. 4E), we attempted to quantify the blood vessel content by immunohistochemical analysis with RECA-1 antibody, which reacts with rat endothelial cell surface antigen. As coordinated with the staining of α-SMA (Fig. 5D), majority of vessels in the lungs of MCT-injected animals was occluded with narrowed lumen, compared with lungs in the sham-operated group. The content of muscularized/occluded vessels was ameliorated by the administration of hCB-MSCs without priming (Fig. 7A, B). Particularly, we found a significant increase in the number of both total and normal vessels in the lungs of the S1P-MSC group, compared with both MCT and MSC + MCT group lungs (Fig. 7).

To examine the effects of S1P-MSC injection on the inflammatory response, we measured the transcripts of several proinflammatory cytokines. The lung tissues in the S1P-MSC group exhibited the reduced expression level of interleukin-1 beta (*Il1b*) and interleukin-6 (*Il6*) (Supplementary Fig. S4). Altogether, our results suggest that the priming of MSC by S1P can induce a microenvironment that is favorable to promote angiogenesis and to protect the inflammation response.

Discussion

Our study findings provide experimental evidence that the priming of human MSCs with S1P or LL-37 can enhance migration, self-renewal, anti-inflammatory, and angiogenic

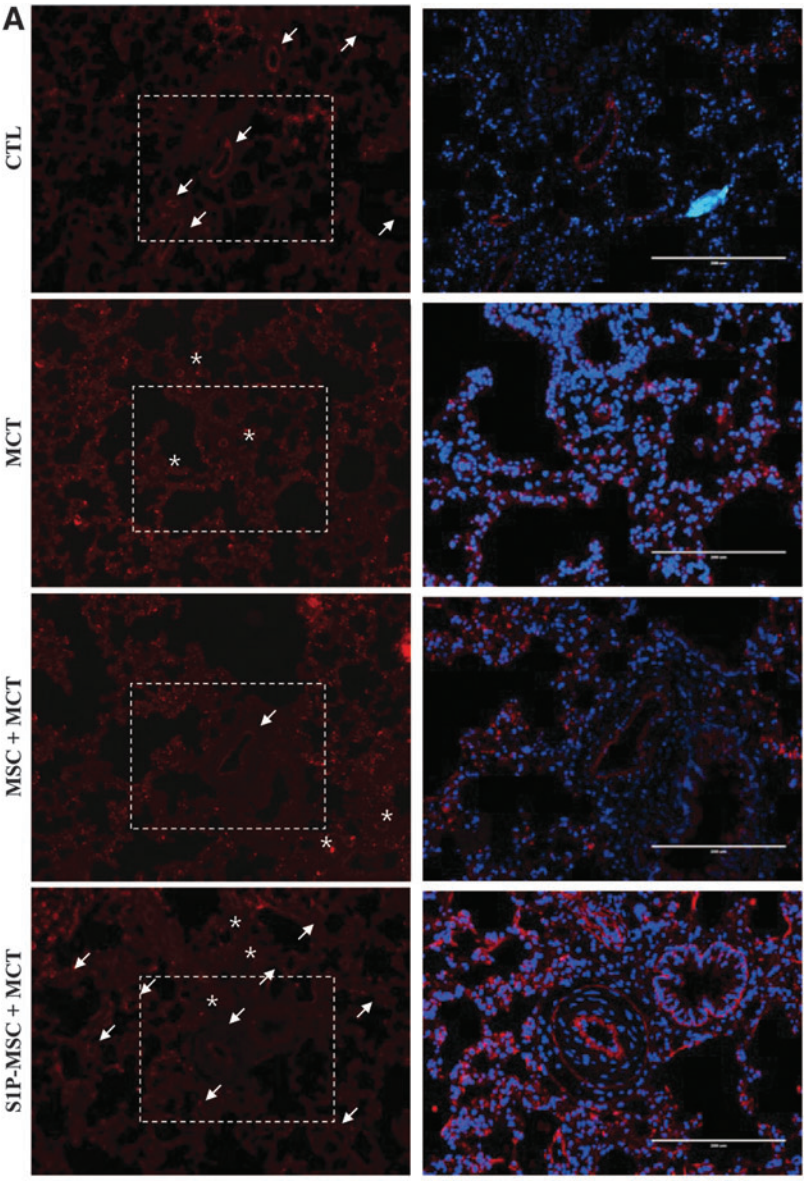

FIG. 7. Increased density of blood vessels in lungs injected with S1P-primed MSC. **(A)** Immunohistochemical detection of rat RECA-1-positive vessels in lung tissues (magnification, $\times 100$). The normal and muscularized/occluded vessels were marked as *arrow* and *asterisk*, respectively. The *boxed area* in *left panel* image is shown in the *right panel* at higher magnification ($\times 200$, scale bar $= 200\,\mu m$). Nuclei were stained with 4′,6-diamidino-2-phenylindole (*blue*). **(B)** The number of RECA-1^+ normal or muscularized (*asterisk*) vessels was assessed from at least 11 randomly selected fields and presented as mean ± SEM. $^{**}P < 0.01$ compared to MCT only (normal vessel), $^{\#\#}P < 0.01$ compared to MCT only (transformed vessel), $^{\$}P < 0.05$ compared to MSC + MCT (normal vessel) (two-way ANOVA with Bonferroni post-test). MSC, hCB-MSC; S1P-MSC, hCB-MSC primed with 0.2 μM S1P for 3 h before injection.

potency, which in turn provides beneficial effects against PAH. Several factors secreted from damaged tissue, such as bioactive lipids and cationic peptides, were found to be strong chemoattractants for several types of tissue-resident adult SCs, including HSPCs and MSCs. Furthermore, our present findings suggest that the priming phenomenon might play a crucial role in the recruitment of these cells during the tissue repair process.

In the chemotaxis assay, hCB-MSCs responded to both S1P and LL-37 more robustly than hAD-MSCs (Fig. 1). This finding could be explained by the different activation status of the MAPKp42/44 and AKT pathways between the

two MSCs (Fig. 2), suggesting that the susceptibility to activation of these signal transduction pathways could determine responsiveness to the priming factors. Recently, it was reported that C1P, a bioactive lipid released from damaged cells (*eg*, heart tissue during acute hypoxia), can chemoattract and stimulate the MAPKp42/44 and AKT pathways in several types of bone marrow (BM)-resident nonhematopoietic SCs, including MSCs, endothelial precursor cells, and very embryonic-like stem cells [36]. Thus, it is conceivable that several factors secreted from damaged organs might create a chemotactic gradient for SCs circulating in PB, and that such cells could be involved in tissue or organ repair. Further studies will be necessary to elucidate the precise role of each priming factor in the mobilization and engraftment of a variety of nonhematopoietic adult SCs during the tissue repair process.

Although S1P and LL-37 have little effect on the basic biology of MSCs, including the cell surface marker phenotype, cell proliferation, and differentiation (Fig. 3), they can stimulate colony forming activity, as estimated by the CFU-F assay (Fig. 4A). Furthermore, in a cell-based anti-inflammatory and angiogenesis assays, CM collected from hCB-MSC repressed the secretion of TNF-α protein from LPS-stimulated alveolar macrophages (Fig. 4B) and enhanced the proliferation of endothelial cells (Fig. 4D). Importantly, these beneficial effects were further enhanced by S1P priming (Fig. 4B, D). The secretion of several trophic, immunosuppressive, anti-inflammatory, and proangiogenic factors by MSCs was responsible for paracrine effects, which significantly contributed to the beneficial outcomes of MSC therapy targeted to several diseases. Particularly, prostaglandin E_2 and TNF-α-stimulated gene/protein-6 are responsible for the anti-inflammatory capacity of MSCs [48,57]. Employing RQ-PCR analysis, we demonstrated that S1P primed hCB-MSCs upregulated the several anti-inflammation (*eg*, *TSG6* and *LIF*) and angiogenic genes (*eg*, *CXCL4*, *HGF*, *PDGFRA*, *VEGFA*, and *ANGPT1*), but at the same time repressed the proinflammation ones (*CCL2*, *IL1B*, and *IL6*). Thus, further in-depth characterization of these S1P-dependent target genes could advance our understanding of the role of bioactive lipids in maintaining tissue homeostasis.

Based on these in vitro results, we then examined the therapeutic potency of hCB-MSC and S1P-primed MSC, which have shown higher migration and clonogenic activity than LL-37 in a MCT-induced PAH model. Furthermore, we proved that S1P-MSCs could successfully improve all parameters related to PAH, including RVSP, RV hypertrophy (RV/LV + S), and pulmonary vascular remodeling (medial wall thickness). Previously, the beneficial effects of murine SCs have been reported in various PAH models [17,58–60]. However, studies of human SC therapies for PAH are limited; only one study reported the effects of human amniotic fluid SCs, which showed anti-inflammatory activities that could be attributed to the immune suppression observed in this study [61]. To translate SC therapy to human clinical trials, it will be important to confirm the effects of human SCs and an appropriate instillation protocol, including cell types, cell abundance, and injection routes. In this context, our study represents a meaningful first step to translating these studies to humans.

Although S1P-MSCs showed some potential in PAH treatment, we should consider several issues before initiating human clinical trials. First, the S1P and its related pathways are reported to promote the proliferation of pulmonary arterial smooth muscle cells, which is a major contributor to pulmonary vascular remodeling [41,62]. By quantification assay, we found that hCB-MSCs under normal culture had low level of S1P; however, the priming of S1P, but not LL-37 significantly increased the S1P content although S1P used for priming was completely removed by extensive washing cells with normal saline solution before injection (Supplementary Fig. S5). Thus, it should carefully monitor the level of S1P left behind priming to exclude the possibility that residual S1P can deteriorate the vasoconstriction in PAH circulation. Second, the genetic and epigenetic instability of SCs represents an obstacle to regenerative medicine, and we should consider the hypothetical risks for tumor development in patients who receive SCs that contain cytogenetic abnormalities [63]. Additional safety data from long-term observations should be obtained before starting human trials. Finally, we should identify more effective methods to maximize the effects of SC therapy, although S1P priming has shown some functional and morphological benefits. Increasing CXCR4 expression in MSCs could represent a possibility [64].

In conclusion, we provide evidence that MSCs exposed to priming factors, such as S1P and LL-37, stimulate beneficial activities of MSCs that can improve the therapeutic potency of these SCs in PAH disorders. Therefore, our findings could provide a novel framework for improving the therapeutic efficacy of adult SC-based therapies for several complex intractable disorders.

Acknowledgments

We thank the NRB (Neuromarker Resource Bank) for providing research information. This research was partly supported by a grant from the Korean Health Technology R&D Project, Ministry of Health and Welfare, Republic of Korea (grant no. A120301) awarded to D.-M.S., S.W.L., (grant no. HI14C3339) awarded to D.-M.S., and (grant no. A120216) awarded to S.W.K., Y.-M.O., and a grant from the Asan Institute for Life Sciences, Asan Medical Center, Seoul, Korea (grant no. 2014-098).

Author Disclosure Statement

No competing financial interests exist.

References

1. Galie N, MM Hoeper, M Humbert, A Torbicki, JL Vachiery, JA Barbera, et al. (2009). Guidelines for the diagnosis and treatment of pulmonary hypertension: the Task Force for the Diagnosis and Treatment of Pulmonary Hypertension of the European Society of Cardiology (ESC) and the European Respiratory Society (ERS), endorsed by the International Society of Heart and Lung Transplantation (ISHLT). Eur Heart J 30:2493–2537.
2. D'Alonzo GE, RJ Barst, SM Ayres, EH Bergofsky, BH Brundage, KM Detre, et al. (1991). Survival in patients with primary pulmonary hypertension. Results from a national prospective registry. Ann Intern Med 115:343–349.
3. Channick RN, G Simonneau, O Sitbon, IM Robbins, A Frost, VF Tapson, et al. (2001). Effects of the dual

endothelin-receptor antagonist bosentan in patients with pulmonary hypertension: a randomised placebo-controlled study. Lancet 358:1119–1123.
4. Olschewski H, G Simonneau, N Galie, T Higenbottam, R Naeije, LJ Rubin, et al. (2002). Inhaled iloprost for severe pulmonary hypertension. N Engl J Med 347:322–329.
5. Simonneau G, RJ Barst, N Galie, R Naeije, S Rich, RC Bourge, et al. (2002). Continuous subcutaneous infusion of treprostinil, a prostacyclin analogue, in patients with pulmonary arterial hypertension: a double-blind, randomized, placebo-controlled trial. Am J Respir Crit Care Med 165:800–804.
6. Galie N, D Badesch, R Oudiz, G Simonneau, MD McGoon, AM Keogh, et al. (2005). Ambrisentan therapy for pulmonary arterial hypertension. J Am Coll Cardiol 46:529–535.
7. Galie N, HA Ghofrani, A Torbicki, RJ Barst, LJ Rubin, D Badesch, et al. (2005). Sildenafil citrate therapy for pulmonary arterial hypertension. N Engl J Med 353:2148–2157.
8. Pulido T, I Adzerikho, RN Channick, M Delcroix, N Galie, HA Ghofrani, et al. (2013). Macitentan and morbidity and mortality in pulmonary arterial hypertension. N Engl J Med 369:809–818.
9. Benza RL, DP Miller, RJ Barst, DB Badesch, AE Frost and MD McGoon. (2012). An evaluation of long-term survival from time of diagnosis in pulmonary arterial hypertension from the REVEAL Registry. Chest 142:448–456.
10. Wang CH, WJ Cherng, NI Yang, LT Kuo, CM Hsu, HI Yeh, et al. (2008). Late-outgrowth endothelial cells attenuate intimal hyperplasia contributed by mesenchymal stem cells after vascular injury. Arterioscler Thromb Vasc Biol 28:54–60.
11. Westerweel PE and MC Verhaar. (2008). Directing myogenic mesenchymal stem cell differentiation. Circ Res 103:560–561.
12. Minguell JJ, C Allers and GP Lasala. (2013). Mesenchymal stem cells and the treatment of conditions and diseases: the less glittering side of a conspicuous stem cell for basic research. Stem Cells Dev 22:193–203.
13. Tashiro K, A Nonaka, N Hirata, T Yamaguchi, H Mizuguchi and K Kawabata. (2014). Plasma elevation of vascular endothelial growth factor leads to the reduction of mouse hematopoietic and mesenchymal stem/progenitor cells in the bone marrow. Stem Cells Dev 23:2202–2210.
14. Karapetyan AV, YM Klyachkin, S Selim, M Sunkara, KM Ziada, DA Cohen, et al. (2013). Bioactive lipids and cationic antimicrobial peptides as new potential regulators for trafficking of bone marrow-derived stem cells in patients with acute myocardial infarction. Stem Cells Dev 22:1645–1656.
15. Gnecchi M, Z Zhang, A Ni and VJ Dzau. (2008). Paracrine mechanisms in adult stem cell signaling and therapy. Circ Res 103:1204–1219.
16. Gnecchi M, H He, N Noiseux, OD Liang, L Zhang, F Morello, et al. (2006). Evidence supporting paracrine hypothesis for Akt-modified mesenchymal stem cell-mediated cardiac protection and functional improvement. FASEB J 20:661–669.
17. Baber SR, W Deng, RG Master, BA Bunnell, BK Taylor, SN Murthy, et al. (2007). Intratracheal mesenchymal stem cell administration attenuates monocrotaline-induced pulmonary hypertension and endothelial dysfunction. Am J Physiol Heart Circ Physiol 292:H1120–H1128.
18. Zhang ZH, Y Lu, Y Luan and JJ Zhao. (2012). Effect of bone marrow mesenchymal stem cells on experimental pulmonary arterial hypertension. Exp Ther Med 4:839–843.
19. Farber HW and J Loscalzo. (2004). Pulmonary arterial hypertension. N Engl J Med 351:1655–1665.
20. Fadini GP, A Avogaro, G Ferraccioli and C Agostini. (2010). Endothelial progenitors in pulmonary hypertension: new pathophysiology and therapeutic implications. Eur Respir J 35:418–425.
21. Price LC, SJ Wort, F Perros, P Dorfmüller, A Huertas, D Montani, et al. (2012). Inflammation in pulmonary arterial hypertension. Chest 141:210–221.
22. Jiang Y, BN Jahagirdar, RL Reinhardt, RE Schwartz, CD Keene, XR Ortiz-Gonzalez, et al. (2002). Pluripotency of mesenchymal stem cells derived from adult marrow. Nature 418:41–49.
23. Oswald J, S Boxberger, B Jorgensen, S Feldmann, G Ehninger, M Bornhauser, et al. (2004). Mesenchymal stem cells can be differentiated into endothelial cells in vitro. Stem Cells 22:377–384.
24. Gehrke I, RK Gandhirajan, SJ Poll-Wolbeck, M Hallek and KA Kreuzer. (2011). Bone marrow stromal cell-derived vascular endothelial growth factor (VEGF) rather than chronic lymphocytic leukemia (CLL) cell-derived VEGF is essential for the apoptotic resistance of cultured CLL cells. Mol Med 17:619–627.
25. Ortiz LA, F Gambelli, C McBride, D Gaupp, M Baddoo, N Kaminski, et al. (2003). Mesenchymal stem cell engraftment in lung is enhanced in response to bleomycin exposure and ameliorates its fibrotic effects. Proc Natl Acad Sci U S A 100:8407–8411.
26. Xu J, CR Woods, AL Mora, R Joodi, KL Brigham, S Iyer, et al. (2007). Prevention of endotoxin-induced systemic response by bone marrow-derived mesenchymal stem cells in mice.Am J Physiol Lung Cell Mol Physiol 293:L131–L141.
27. Ratajczak MZ, E Zuba-Surma, M Kucia, R Reca, W Wojakowski and J Ratajczak. (2006). The pleiotropic effects of the SDF-1-CXCR4 axis in organogenesis, regeneration and tumorigenesis. Leukemia 20:1915–1924.
28. Kucia M, R Reca, K Miekus, J Wanzeck, W Wojakowski, A Janowska-Wieczorek, et al. (2005). Trafficking of normal stem cells and metastasis of cancer stem cells involve similar mechanisms: pivotal role of the SDF-CXCR1–CXCR4 axis. Stem Cells 23:879–894.
29. Tsuzuki Y, D Fukumura, B Oosthuyse, C Koike, P Carmeliet and RK Jain. (2000). Vascular endothelial growth factor (VEGF) modulation by targeting hypoxia-inducible factor-1alpha→hypoxia response element→VEGF cascade differentially regulates vascular response and growth rate in tumors. Cancer Res 60:6248–6252.
30. Morikawa S, Y Mabuchi, Y Kubota, Y Nagai, K Niibe, E Hiratsu, et al. (2009). Prospective identification, isolation, and systemic transplantation of multipotent mesenchymal stem cells in murine bone marrow. J Exp Med 206:2483–2496.
31. Corpechot C, V Barbu, D Wendum, N Chignard, C Housset, R Poupon, et al. (2002). Hepatocyte growth factor and c-met inhibition by hepatic cell hypoxia: a potential mechanism for liver regeneration failure in experimental cirrhosis. Am J Pathol 160:613–620.
32. Kucia M, YP Zhang, R Reca, M Wysoczynski, B Machalinski, M Majka, et al. (2005). Cells enriched in markers of neural tissue-committed stem cells reside in the bone

marrow and are mobilized into the peripheral blood following stroke. Leukemia 20:18–28.
33. Ratajczak MZ, CH Kim, W Wojakowski, A Janowska-Wieczorek, M Kucia and J Ratajczak. (2010). Innate immunity as orchestrator of stem cell mobilization. Leukemia 24:1667–1675.
34. Ratajczak MZ, H Lee, M Wysoczynski, W Wan, W Marlicz, MJ Laughlin, et al. (2010). Novel insight into stem cell mobilization-plasma sphingosine-1-phosphate is a major chemoattractant that directs the egress of hematopoietic stem progenitor cells from the bone marrow and its level in peripheral blood increases during mobilization due to activation of complement cascade/membrane attack complex. Leukemia 24:976–985.
35. Kim CH, W Wu, M Wysoczynski, A Abdel-Latif, M Sunkara, A Morris, et al. (2012). Conditioning for hematopoietic transplantation activates the complement cascade and induces a proteolytic environment in bone marrow: a novel role for bioactive lipids and soluble C5b-C9 as homing factors. Leukemia 26:106–116.
36. Kim C, G Schneider, A Abdel-Latif, K Mierzejewska, M Sunkara, S Borkowska, et al. (2013). Ceramide-1-phosphate regulates migration of multipotent stromal cells and endothelial progenitor cells—implications for tissue regeneration. Stem Cells 31:500–510.
37. Reca R, D Cramer, J Yan, MJ Laughlin, A Janowska-Wieczorek, J Ratajczak, et al. (2007). A novel role of complement in mobilization: immunodeficient mice are poor granulocyte-colony stimulating factor mobilizers because they lack complement-activating immunoglobulins. Stem Cells 25:3093–3100.
38. Ratajczak J, R Reca, M Kucia, M Majka, DJ Allendorf, JT Baran, et al. (2004). Mobilization studies in mice deficient in either C3 or C3a receptor (C3aR) reveal a novel role for complement in retention of hematopoietic stem/progenitor cells in bone marrow. Blood 103:2071–2078.
39. Wu W, CH Kim, R Liu, M Kucia, W Marlicz, N Greco, et al. (2012). The bone marrow-expressed antimicrobial cationic peptide LL-37 enhances the responsiveness of hematopoietic stem progenitor cells to an SDF-1 gradient and accelerates their engraftment after transplantation. Leukemia 26:736–745.
40. Lee HM, W Wu, M Wysoczynski, R Liu, EK Zuba-Surma, M Kucia, et al. (2009). Impaired mobilization of hematopoietic stem/progenitor cells in C5-deficient mice supports the pivotal involvement of innate immunity in this process and reveals novel promobilization effects of granulocytes. Leukemia 23:2052–2062.
41. Chen J, H Tang, JR Sysol, L Moreno-Vinasco, KM Shioura, T Chen, et al. (2014). The sphingosine kinase 1/sphingosine-1-phosphate pathway in pulmonary arterial hypertension. Am J Respir Crit Care Med 190:1032–1043.
42. Rhodes CJ, LS Howard, M Busbridge, D Ashby, E Kondili, JSR Gibbs, et al. (2011). Iron deficiency and raised hepcidin in idiopathic pulmonary arterial hypertension: clinical prevalence, outcomes, and mechanistic insights. J Am Coll Cardiol 58:300–309.
43. Song M, J Heo, JY Chun, HS Bae, JW Kang, H Kang, et al. (2014). The paracrine effects of mesenchymal stem cells stimulate the regeneration capacity of endogenous stem cells in the repair of a bladder-outlet-obstruction-induced overactive bladder. Stem Cells Dev 23:654–663.
44. Lee M, SY Jeong, J Ha, M Kim, HJ Jin, S-J Kwon, et al. (2014). Low immunogenicity of allogeneic human umbilical cord blood-derived mesenchymal stem cells in vitro and in vivo. Biochem Biophys Res Commun 446:983–989.
45. Jang YK, M Kim, Y-H Lee, W Oh, YS Yang and SJ Choi. (2014). Optimization of the therapeutic efficacy of human umbilical cord blood–mesenchymal stromal cells in an NSG mouse xenograft model of graft-versus-host disease. Cytotherapy 16:298–308.
46. Dominici M, K Le Blanc, I Mueller, I Slaper-Cortenbach, F Marini, D Krause, et al. (2006). Minimal criteria for defining multipotent mesenchymal stromal cells. The International Society for Cellular Therapy position statement. Cytotherapy 8:315–317.
47. Yu K-R, S-R Yang, J-W Jung, H Kim, K Ko, DW Han, et al. (2012). CD49f enhances multipotency and maintains stemness through the direct regulation of OCT4 and SOX2. Stem Cells 30:876–887.
48. Bartosh TJ, JH Ylöstalo, A Mohammadipoor, N Bazhanov, K Coble, K Claypool, et al. (2010). Aggregation of human mesenchymal stromal cells (MSCs) into 3D spheroids enhances their antiinflammatory properties. Proc Natl Acad Sci U S A 107:13724–13729.
49. Staton CA, MWR Reed and NJ Brown. (2009). A critical analysis of current in vitro and in vivo angiogenesis assays. Int J Exp Pathol 90:195–221.
50. van Suylen RJ, WM Aartsen, JF Smits and MJ Daemen. (2001). Dissociation of pulmonary vascular remodeling and right ventricular pressure in tissue angiotensin-converting enzyme-deficient mice under conditions of chronic alveolar hypoxia. Am J Respir Crit Care Med 163:1241–1245.
51. Minamino T, H Christou, CM Hsieh, Y Liu, V Dhawan, NG Abraham, et al. (2001). Targeted expression of heme oxygenase-1 prevents the pulmonary inflammatory and vascular responses to hypoxia. Proc Natl Acad Sci U S A 98:8798–8803.
52. Shin DM, EK Zuba-Surma, W Wu, J Ratajczak, M Wysoczynski, MZ Ratajczak, et al. (2009). Novel epigenetic mechanisms that control pluripotency and quiescence of adult bone marrow-derived Oct4 + very small embryonic-like stem cells. Leukemia 23:2042–2051.
53. Bae SH, HS Lee, MS Kang, BJ Strupp, M Chopp and J Moon. (2012). The levels of pro-inflammatory factors are significantly decreased in cerebral palsy patients following an allogeneic umbilical cord blood cell transplant. Int J Stem Cells 5:31–38.
54. Cheng AS and TM Yau. (2008). Paracrine effects of cell transplantation: strategies to augment the efficacy of cell therapies. Semin Thorac Cardiovasc Surg 20:94–101.
55. Maltais S, J Tremblay, L Perrault and H Ly. (2010). The paracrine effect: pivotal mechanism in cell-based cardiac repair. J Cardiovasc Transl Res 3:652–662.
56. Gharaibeh B, M Lavasani, J Cummins and J Huard. (2011). Terminal differentiation is not a major determinant for the success of stem cell therapy—cross-talk between muscle-derived stem cells and host cells. Stem Cell Res Ther 2:31.
57. Bartosh TJ, JH Ylöstalo, N Bazhanov, J Kuhlman and DJ Prockop. (2013). Dynamic compaction of human mesenchymal stem/precursor cells into spheres self-activates caspase-dependent IL1 signaling to enhance secretion of modulators of inflammation and immunity (PGE2, TSG6, and STC1). Stem Cells 31:2443–2456.
58. Lee C, SA Mitsialis, M Aslam, SH Vitali, E Vergadi, G Konstantinou, et al. (2012). Exosomes mediate the cytoprotective action of mesenchymal stromal cells on

hypoxia-induced pulmonary hypertension. Circulation 126:2601–2611.
59. Liang OD, SA Mitsialis, MS Chang, E Vergadi, C Lee, M Aslam, et al. (2011). Mesenchymal stromal cells expressing heme oxygenase-1 reverse pulmonary hypertension. Stem Cells 29:99–107.
60. Zhao YD, DW Courtman, Y Deng, L Kugathasan, Q Zhang and DJ Stewart. (2005). Rescue of monocrotaline-induced pulmonary arterial hypertension using bone marrow-derived endothelial-like progenitor cells: efficacy of combined cell and eNOS gene therapy in established disease. Circ Res 96:442–450.
61. Angelini A, C Castellani, B Ravara, C Franzin, M Pozzobon, R Tavano, et al. (2011). Stem-cell therapy in an experimental model of pulmonary hypertension and right heart failure: role of paracrine and neurohormonal milieu in the remodeling process. J Heart Lung Transplant 30:1281–1293.
62. Ota H, MA Beutz, M Ito, K Abe, M Oka and IF McMurtry. (2011). S1P4 receptor mediates S1P-induced vasoconstriction in normotensive and hypertensive rat lungs. Pulm Circ 1:399–404.
63. Barkholt L, E Flory, V Jekerle, S Lucas-Samuel, P Ahnert, L Bisset, et al. (2013). Risk of tumorigenicity in mesenchymal stromal cell-based therapies—bridging scientific observations and regulatory viewpoints. Cytotherapy 15:753–759.
64. Jones GN, D Moschidou, K Lay, H Abdulrazzak, M Vanleene, SJ Shefelbine, et al. (2012). Upregulating CXCR4 in human fetal mesenchymal stem cells enhances engraftment and bone mechanics in a mouse model of osteogenesis imperfecta. Stem Cells Transl Med 1:70–78.

Address correspondence to:
Dong-Myung Shin, PhD
Department of Biomedical Sciences
Asan Medical Center
University of Ulsan College of Medicine
Pungnap-2 dong, Songpa-gu
Seoul 138-736
Korea

E-mail: d0shin03@amc.seoul.kr

Sei Won Lee, MD, PhD
Department of Pulmonary and Critical Care Medicine, and Clinical Research Center for Chronic Obstructive Airway Diseases
Asan Medical Center
University of Ulsan College of Medicine
Pungnap-2 dong, Songpa-gu
Seoul 138-736
Korea

E-mail: iseiwon@gmail.com

Received for publication October 20, 2014
Accepted after revision March 11, 2015
Prepublished on Liebert Instant Online March 11, 2015